Contents lists available at ScienceDirect

# Composites Science and Technology

journal homepage: www.elsevier.com/locate/compscitech

# Experimental optimization of the impact energy absorption of epoxy–carbon laminates through controlled delamination

Alessandro Pegoretti *, Ivan Cristelli, Claudio Migliaresi

*Department of Materials Engineering and Industrial Technologies and INSTM Research Unit, University of Trento, via Mesiano 77, 38100 Trento, Italy*

ABSTRACT

In this paper, the correlation between interlaminar fracture toughness and impact energy absorption for the fracture of epoxy–carbon laminates was studied. Carbon fibres–epoxy cross-ply prepreg layers were interleaved with thin (26 μm) poly(ethylene-terephthalate) (PET) films. Before the composite preparation, circular holes 1 mm in diameter were drilled in the PET films at several densities (from 0 up to 44 holes/cm$^2$) in order to selectively increase the interlaminar contact area between the epoxy–carbon laminae. In this way, the interlaminar contact area was gradually varied from 0%, corresponding to the case in which non-perforated PET films were used, up to 100% in the case of non-interleaved laminates. The Mode I interlaminar fracture toughness of the resulting laminates was determined according to the ASTM D-5528-01 standard test method on double cantilever beam (DCB) specimens. The critical values of the strain energy release rate determined at the point at which the load versus opening displacement curve becomes non-linear ($G_{IC,NL}$) resulted to vary from 40 up to 260 J/m$^2$, depending on the interlaminar contact area. All the laminates were then characterized by three point bending tests performed both under quasi-static (5 mm/min) and impact (2 m/s) loading conditions. The elastic modulus of the laminates resulted to be practically independent of the level of interlaminar adhesion, while the bending strength decreased as the interlaminar fracture toughness decreased. The total energy to fracture evaluated under impact conditions showed a non-monotonic correlation with the interlaminar fracture toughness, reaching a maximum level in correspondence of a $G_{IC,NL}$ value of about 60 J/m$^2$. At the same time, the ductility index, i.e. the ratio between the propagation and the initiation energies, evaluated by instrumented Charpy impact tests, markedly increased as the interlaminar fracture toughness decreased.

© 2008 Elsevier Ltd. All rights reserved.

## 1. Introduction

The potential for weight savings with fiber-reinforced composites renders these materials very attractive for several structural application areas, which include military, aircraft, space, automotive, marine and sporting goods applications [1]. Many fibre-reinforced composite materials offer a combination of specific modulus and strength values that are either comparable to or better than many traditional metallic materials [1]. For some specific components, such as bumpers, armours, helmets, disposable barrier shells, etc., the most important material requirement is the capacity to absorb a large amount of mechanical energy under impact conditions before reaching complete fracture. Most composites are brittle and so can only absorb energy in elastic deformation and through damage mechanisms, and not via plastic deformation [2]. There are five basic mechanical failure modes that can occur in a composite after the initial elastic deformation [3]: (i) fibre fracture, or, for aramids, defibrilation, (ii) resin crazing, micro-cracking and gross fracture, (iii) debonding between fibre and matrix, (iv) fibre pull out from the matrix, and (v) delamination of adjacent plies in a laminate. In general, each of the above mentioned mechanisms may contribute to the energy dissipation process under impact conditions. Delamination is the most important damage mechanism in impacted composite laminates [4]. When a composite structure is impacted, delamination often occurs, which seriously reduces the load bearing capacity of the laminate especially under compressive loads [5]. Therefore, several methods have been developed to improve the interlaminar strength and interlaminar fracture toughness of composite laminates, such as matrix toughening [6–9], through-thickness stitching [10–14], Z-pinning [15,16], interleaving [17–25] and short-fibre interlaminar reinforcement [25]. Most of the above mentioned methods have been reviewed by Kim and Mai [26], who also pointed out the key role played by the fibre–matrix interfacial shear strength in determining the interlaminar resistance of composite laminates. In fact, a marked improvement of the interlaminar resistance when the fibre–matrix adhesion increases is reported in several studies [27–30]. On the other hand, the improvement of damage resistance and tolerance in interlaminar fracture is at the expenses of other

important mechanical properties, such as the energy absorption under impact conditions [31] and the fatigue resistance. In fact, as the interlaminar strength increases the delamination damage is hindered, and the composite laminates tend to fracture in a more brittle way under impact conditions. Hong and Liu [32] showed that there is an almost linear relationship between the impact energy and the total delaminated area in glass/epoxy laminates. As a consequence, an efficient way to improve the energy absorption capacity of laminate composites in the through-thickness direction is to promote controlled delamination by weakening the interlaminar bond strength or interlaminar fracture toughness [26]. The transverse Charpy impact fracture energy of carbon fibre reinforced plastics (CFRPs) has been successfully increased by three times with embedded nylon sheets, at the expenses of some 25% reduction of the interlaminar shear strength [33]. Perforated films have been proven to be more effective than unperforated ones because they could provide both the weak and strong bonding in the regions of film and perforation ("intermittent interlaminar bond concept" [34]). In fact, using multi-layers of perforated Mylar films, Jea and Felbeck [35] reached a remarkable 500% increase of the transverse fracture toughness (determined on reinforced modified compact tension specimens) of CFRPs, while the tensile transverse strength dropped about 20% and the Young's modulus remained the same. The transverse fracture toughness was determined by Jang et al. [36] on fibrous composites with several other types of delamination promoters, including aluminium foils, bleached papers, polyester textile fabrics and polyimide Mylar. They found that the energy absorption mechanisms strongly depend on the loading direction and other testing parameters such as loading speed and span-to-depth ratio in bending. Moreover, the existence of an optimal value of the interlaminar fracture toughness corresponding to maximum energy absorption has been theoretically proven by Lear and Sankar [37], but not experimentally verified. Delamination, and therefore the energy absorbing capability, of composite laminates has been also successfully promoted by other techniques, such as the introduction of fibre orientation change between adjacent layers [32], the modification of the target stiffness [38], or the introduction of ply grouping [39].

Aiming at optimizing the energy absorption capability of carbon/epoxy laminates under impact conditions, in the present work the "intermittent interlaminar bond concept" has been further explored. In particular, the possibility to selectively change the interlaminar fracture toughness by interleaving with poly(ethylene-terephthalate) foils perforated with a variable number of holes per unit area (hole density), has been investigated, and its effects on the composites impact behaviour have been assessed.

## 2. Experimental

### 2.1. Materials

Carbon fibre/epoxy resin cross-ply prepreg (CC 206–ET443) was supplied by SEAL S.p.A. Legnano (MI), Italy. The carbon fabric (CC 206) consisted of high strength carbon yarns (HS 3K) in a twill 2/2 weave with a weight of 204 g/m$^2$ (102 g/m$^2$ in the warp and 102 g/m$^2$ in the weft directions). The matrix (ET443) was a transparent epoxy resin with a gel time of $9 \pm 3$ min, a cured density of 1.2 g/cm$^3$, and a fully cured glass transition temperature of about 145 °C.

Mylar® (DuPont) poly(ethylene-terephthalate) (PET) foils, 26 μm thick, were used as interleaving material. These foils displayed in-plane isotropic mechanical properties (with a tensile modulus of 4.5 GPa, and a yield strength of 97.2 MPa), a glass transition temperature of 105 °C, a melting temperature of 260 °C, and a crystallinity content of about 36% [40].

### 2.2. Composites manufacturing

By using a computer-controlled high-speed drill the PET foils were perforated with circular holes 1 mm in diameter (see Fig. 1a). Holes were regularly spaced at a distance L, as schematized in Fig. 1b. As the distance L varied from 7 to 1.5 mm, the hole density changed from 2.0 up to 44.4 holes/cm$^2$), according to Table 1. The interfacial contact area (ICA) is obviously related to the hole density and it can be estimated as follows:

$$ICA = \frac{\pi}{4}\left(\frac{D}{L}\right)^2 \tag{1}$$

The relationship between the parameter ICA and the hole density is reported in Table 1. Before to be used for composite preparation, both as-received and perforated PET foils were accurately washed with water and a detergent, and then rinsed, first in water and finally in n-heptane.

The prepreg laminae were cut in size of $150 \times 150$ mm$^2$ and non-interleaved or interleaved composites were realized by alternating prepreg laminae and PET foils according to the stacking sequences schematized in Fig. 2. It is worth noting that an ICA value of 100% can be assigned to the non-interleaved composites, while a
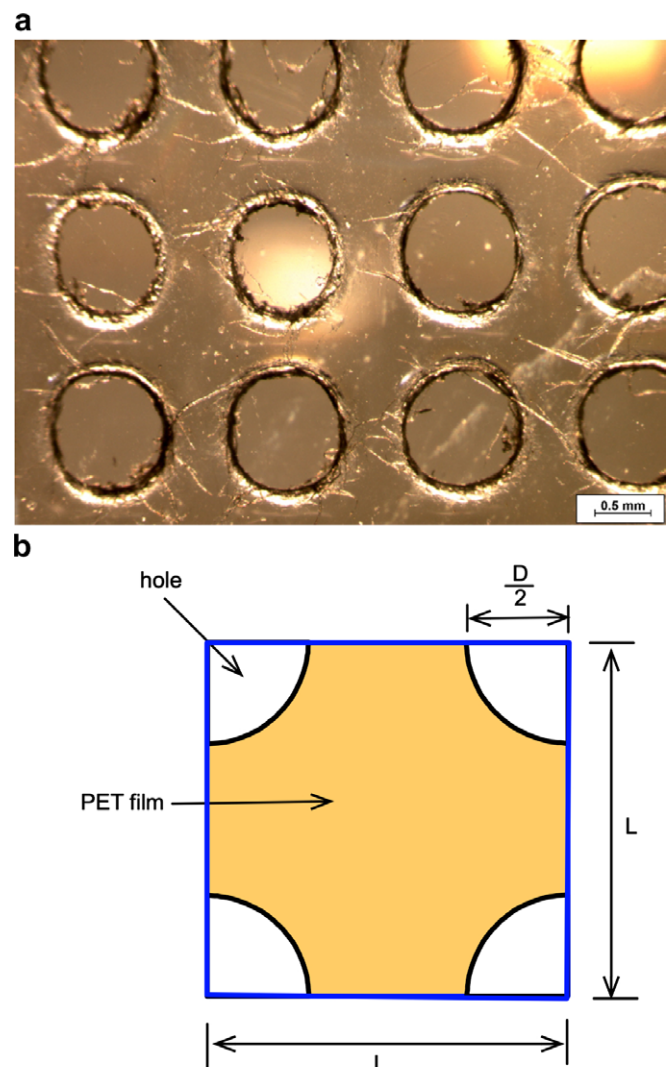


**Fig. 1.** Perforated PET foil: (a) optical micrograph and (b) schematic of the hole distribution.

**Table 1**
Relationship between the inter-hole distance ($L$), the hole density, and the interfacial contact area (ICA)

| Inter-hole distance $L$ (mm) | Hole density (number of holes/cm$^2$) | Interfacial contact area ICA (%) |
|---|---|---|
| No holes | 0.0 | 0.0 |
| 7.0 | 2.0 | 1.6 |
| 6.0 | 2.8 | 2.2 |
| 5.0 | 4.0 | 3.1 |
| 4.0 | 6.3 | 4.9 |
| 3.0 | 11.1 | 8.7 |
| 2.5 | 16.0 | 12.6 |
| 2.0 | 25.0 | 19.6 |
| 1.5 | 44.4 | 34.9 |
| No PET foils | | 100.0 |

0% ICA value can be considered for the composites interleaved with non-perforated PET foils. By using perforated PET foils the interfacial contact area can be gradually varied in the range reported in Table 1. The number of stacked laminae was also changed depending on the type of test to perform (see following sections). All the prepreg fabrics were stacked with the same relative orientation.

The curing cycle presented in Fig. 3 was adopted for the composite consolidation.

### 2.3. Interlaminar fracture toughness test

Mode I interlaminar fracture toughness ($G_{IC}$) was measured on double cantilever beam (DCB) specimens whose geometry is reported in Fig. 4. According to ASTM D-5528-01 standard the following dimensions were adopted: $L$ = 135 mm; $b$ = 25 mm; $a_0$ =

50 mm; $h$ = 3.00–3.90 mm. Non-interleaved specimens were prepared by stacking 16 prepreg laminae, while interleaved specimens were prepared by alternating 16 prepreg laminae with 15 PET foils. A non-adhesive fluoroethylene-propylene foil (Teflon$^®$ FEP – DuPont) with a thickness of about 25 μm was inserted at the midplane of the laminates during layup to form an initiation site for the delamination. After cutting the DCB specimens to the desired size, piano hinges were bonded by a room temperature curable bicomponent epoxy resin. Delamination tests were performed at room temperature by an Instron 4502 universal testing machine at a cross-head speed of 2 mm/min recording the experiments by a digital video-camera. According to one of the data reduction methods proposed by the ASTM D-5528-01 standard, $G_{IC}$ value has been calculated as follows:

$$G_{IC} = \frac{nP\delta}{2ba} \tag{2}$$

where $P$ is the load, $\delta$ is the load point displacement, and the coefficient $n$ is evaluated through a compliance calibration method. This method is based on the construction of a plot of $\log(\delta_i/P_i)$ versus $\log(a_i)$ using the visually observed delamination onset values and all the propagation values as represented in Fig. 5a: $n$ represents the slope of the least square linear regression line passing through the data. As reported in Fig. 5b the obtained $n$ values resulted to be practically independent of the interlaminar contact area with values oscillating around 2.5.

### 2.4. Three point bending test

According to ASTM D-790-03 standard, three point bending tests were performed on composite bars with a thickness of
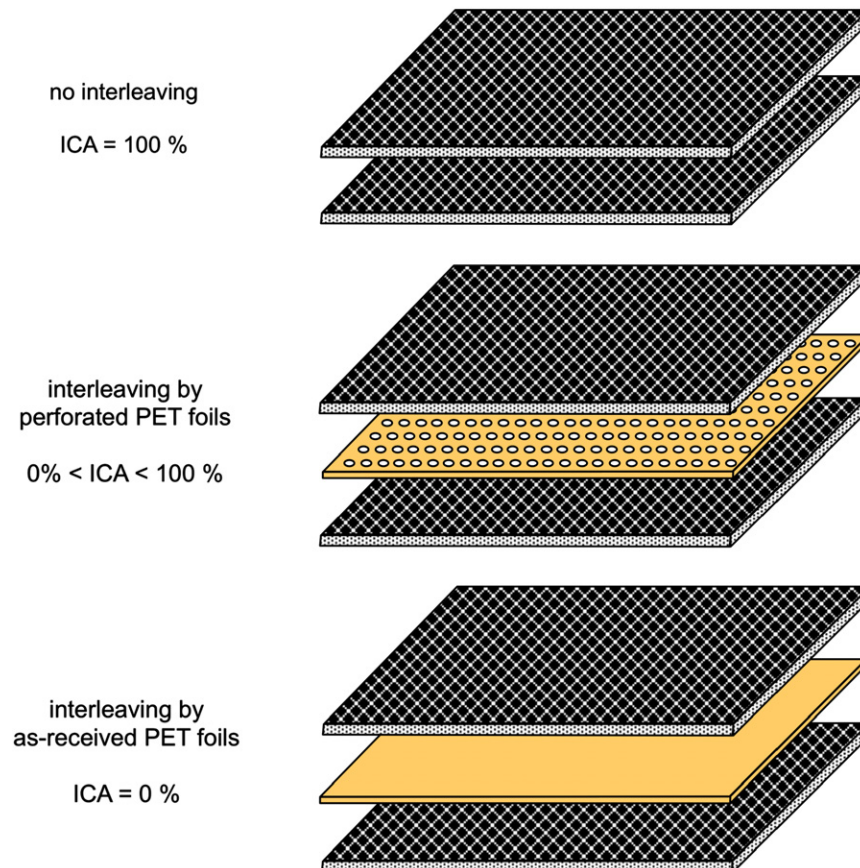


no interleaving
ICA = 100 %

interleaving by perforated PET foils
0% < ICA < 100 %

interleaving by as-received PET foils
ICA = 0 %

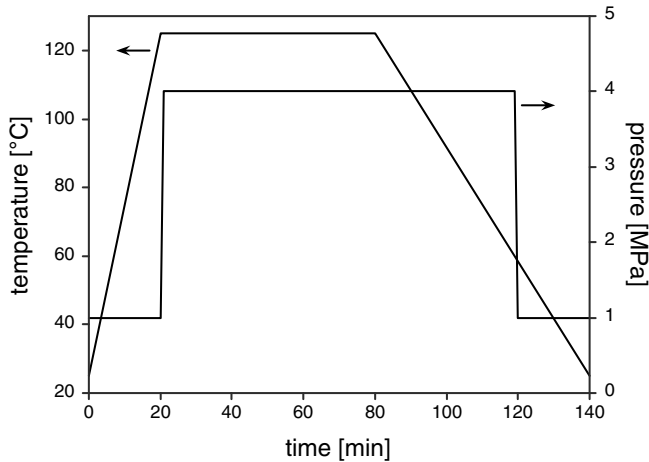Fig. 2. Stacking sequences of the non-interleaved and PET-interleaved laminates.

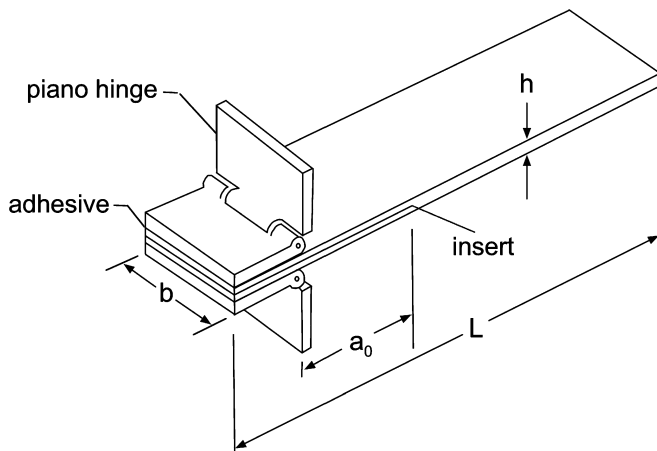**Fig. 3.** Temperature and pressure profiles adopted for the composites curing cycle.



**Fig. 4.** Schematic of the DCB specimens.



**Fig. 5.** (a) Typical compliance calibration plot and (b) n exponent as a function of the interlaminar contact area.

1.7 mm, a width of 12.7 mm and a length of 110 mm. The test bars were machined out of composite plates consisting of eight prepreg laminae (non-interleaved composites) or of eight prepreg laminae interleaved with seven PET foils. Load–deflection curves were obtained at room temperature by an Instron 4502 machine at a cross-head speed of 5 mm/min at a span length of 80 mm. At least five specimens were tested for each sample. According to ASTM D-790-03 standard, a bending modulus, $E_b$, and a bending strength, $\sigma_b$, were calculated by using the following formulae:

$$E_b = \frac{S^3 m}{4bd^3} \tag{3}$$

$$\sigma_b = \frac{3P_{max}S}{2bd^2} \tag{4}$$

where $S$ is the span length, $b$ the width and $d$ the thickness of the specimen, $P_{max}$, the maximum measured load, and $m$ the slope of the tangent to the initial straight-line portion of the load–deflection curve.

### 2.5. Instrumented Charpy impact test

Instrumented Charpy impact tests were performed on test bars of rectangular cross section, 80 mm long, 10 mm wide and 1.7 mm thick machined from the same laminates where specimens for three point bending test were o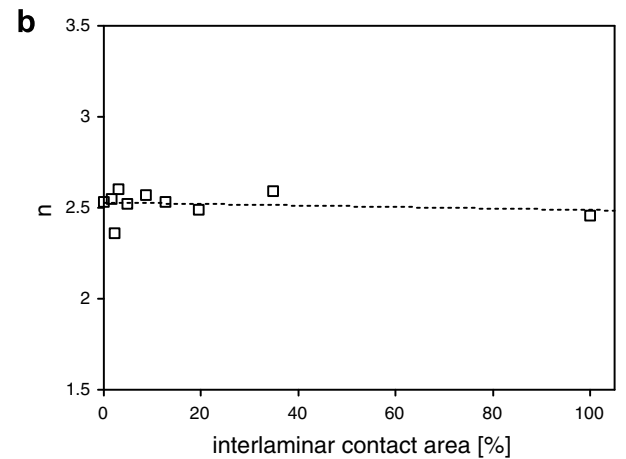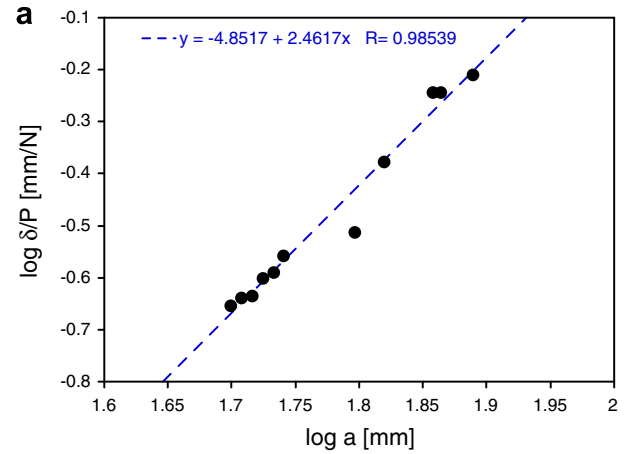btained from. Tests were performed by a CEAST model 6549 instrumented impact pendulum. Specimens were supported to the machine anvils at a span length of 40 mm and broken by a single swing of the pendulum with the impact line midway between the supports in the flat wise direction. The striking nose of the pendulum was characterized by an included angle of 30° and a tip rounded to a radius of 2 mm. The striking hammer impacted the specimens at a speed of 2 m/s and with a kinetics energy of 1.91 J. Load-time data points were acquired at a sampling time of 0.01 ms. At least 10 specimens were tested for each sample.

All the acquired load-time curves were elaborated by the CEAST software DAS4000 Extended Win Acquisition System ver. 3.30 in order to obtain the load–displacement and energy–displacement curves.

Bending modulus, $E_b$, and bending strength, $\sigma_b$, under impact conditions were calculated on the basis of Eqs. (3) and (4), respectively.

## 3. Results and discussion

### 3.1. Interlaminar fracture toughness

Optical micrographs of the cross section of composites, interleaved with both as-received and perforated PET foils, are reported in Fig. 6. In Fig. 6a it is very easy to identify the presence of the as-received (unperforated) PET interleaving foils separating the composite laminae. When perforated PET foils are used the typical composite structure is depicted in Fig. 6b and c, in which the black

arrows indicate the borders of a hole in the PET foils. In most cases, the epoxy matrix was able to flow through the holes in the interleaving foils during composite preparation, as represented in Fig. 6b, thus forming a resin bridge between two adjacent composite laminae. The number of these resin bridges obviously increases with the number of holes per unit area, and hence the interlaminar contact area (ICA), increases. In a few cases (upper and lower parts of Fig. 6c) the resin was not able to flow completely through the holes, and micro-voids were created in the laminate.
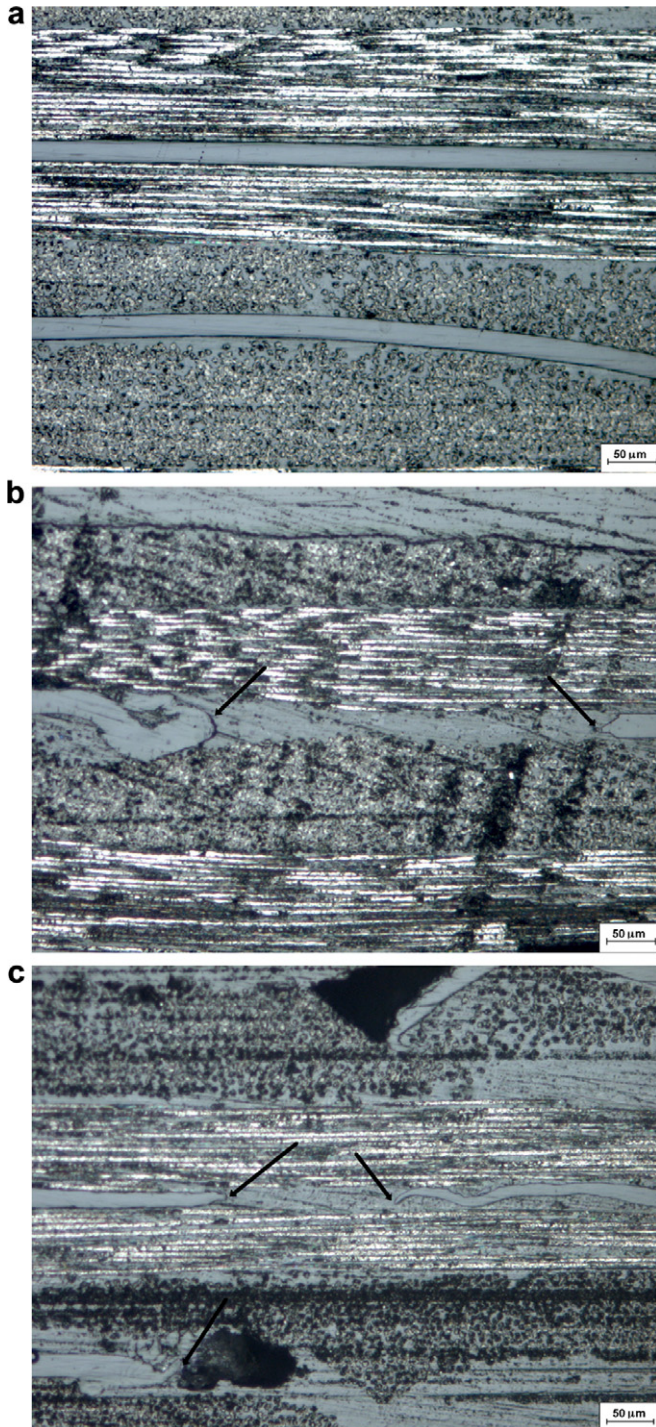


**Fig. 6.** Optical micrographs of the cross section of composites interleaved with (a) as-received, (b) and (c) perforated PET foils (ICA = 19.6%).
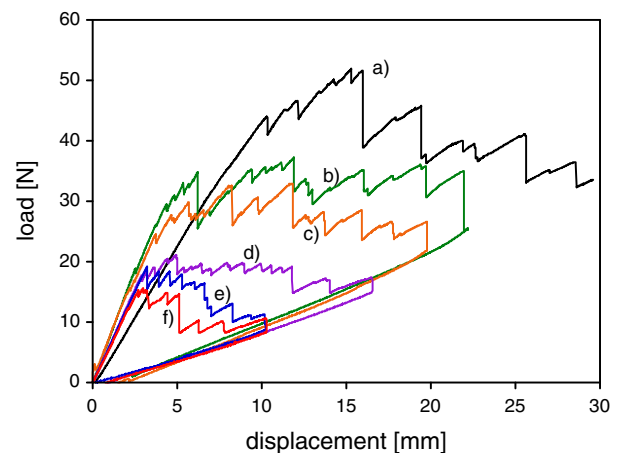
The load–displacement curves for DCB delamination tests performed on composites with various interlaminar contact areas are compared in Fig. 7. It is interesting to observe that these curves tends to reach higher load values as the interlaminar contact area (and hence the number of resin bridges per unit area) increases. According to the data reduction procedures suggested by ASTM standard D-5528-01, an initiation $G_{IC}$ value can be determined using the load and deflection data measured at the point of deviation from linearity in the load–displacement curve ($G_{IC,NL}$), or at the point at which delamination is visually observed ($G_{IC,VIS}$) on the edge of the DCB specimen:

$$G_{IC,NL} = \frac{nP_{NL}\delta_{NL}}{2ba} \tag{5}$$

$$G_{IC,VIS} = \frac{nP_{VIS}\delta_{VIS}}{2ba} \tag{6}$$

where the symbols have the same meaning as in Eq. (2) with the subscripts NL and VIS referring to the point of deviation from linearity in the load–displacement curve and to the point at which delamination is visually observed, respectively. The initiation $G_{IC}$ values obtained using Eqs. (5) and (6) are reported in Fig. 8 as a function of the interlaminar contact area of the laminates. As expected, the interlaminar toughness values for fracture initiation increase as the interlaminar contact area increase, due to the increasing numbers of interlaminar resin bridges. It is worth observing that, independently of the data reduction method, the initiation interlaminar fracture toughness of the composites interleaved with as-received PET foils (ICA = 0%) assumes a value of about 40 J/m². This indicates a relatively good adhesion level between the PET foils and the epoxy matrix. $G_{IC,VIS}$ and $G_{IC,NL}$ values are very similar up to interlaminar contact areas of about 40%, while they markedly differ for the non-interleaved composites which display $G_{IC,NL}$ and $G_{IC,VIS}$ values of about 260 J/m² and 430 J/m², respectively. In the continuation of this article we will refer to $G_{IC,NL}$ values since the underlying data reduction method is more straightforward. From the data reported in Fig. 9 it is possible to observe that the interlaminar contact area also markedly affects the delamination resistance curves. In fact, as the interlaminar contact area decreases $R$ curves tend to flatten and level off at progressively lower limiting values. For low ICA values the delamination resistance is practically independent of the crack length.

At this point, before to present the results of quasi-static and impact tests, it is important to underline that we are conscious that three point bending tests carried out on unnotched specimens are mostly characterized by a sliding mode (Mode II) rather than an



**Fig. 7.** Load–displacement curves for DCB delamination tests performed on composites with various interlaminar contact areas: (a) ICA = 100%, (b) ICA = 34.9%, (c) ICA = 12.6%, (d) ICA = 8.7%, (e) ICA = 3.1%, (f) ICA = 0%.
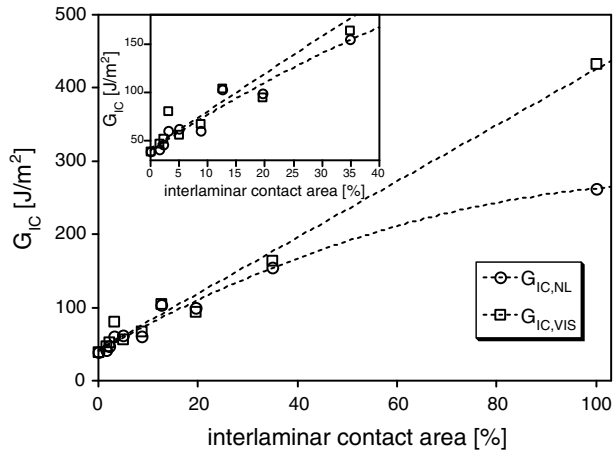
**Fig. 8.** Mode I interlaminar fracture toughness evaluated at first deviation from linearity ($\bigcirc$, $G_{IC,NL}$) and at visual onset of delamination ($\square$, $G_{IC,VIS}$), as a function of the interlaminar contact area.
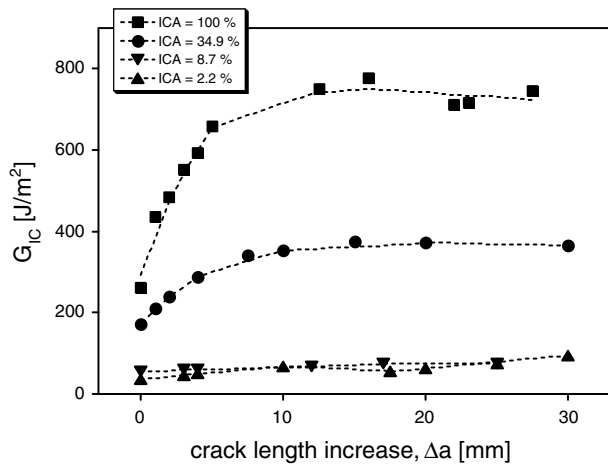


**Fig. 9.** Effect of the interlaminar contact area on the delamination resistance curve ($R$ curve).

opening mode (Mode I). Unfortunately, there is no European nor ASTM mode II standard at present, but the JIS group has a mode II test procedure based on the ENF specimen and an option to allow stabilising the test [41]. At the same time, it is worthwhile to note that most of the experimental data available in the scientific literature indicate that a monotonic relationship exists between Mode I and Mode II interlaminar fracture toughness. In other words, with only few exceptions [42,43], when Mode I interlaminar fracture toughness increases, Mode II interlaminar fracture toughness generally does the same [20,21,44–49]. An estimation of the interlaminar shear strength (ISS) by the short-beam shear test (ASTM D 2344) was also considered, but the small specimens dimensions required for this testing procedure posed a serious limitation on the usefulness of this test for the materials under investigation. In fact, according to ASTM D 2344 standard, specimen with span-to-thickness and a width-to-thickness ratios of 4 and 2, respectively are required. This would have lead to samples with as low as 1–2 resin bridges per lamina, in the case of composites interleaved with foils having the lowest holes densities. As a consequence, the specimens would have not been representative of the situation at a macro scale, like that encountered in quasi-static and impact three point bending tests. On the basis of the above considerations, $G_{IC}$ value

has been preferred as a parameter representative of the interlaminar fracture toughness.

### 3.2. Quasi-static mechanical tests

The mechanical behaviour under quasi-static loading conditions has been investigated by three point bending tests whose results are summarized in Fig. 10a. In this figure, the bending modulus, $E_b$, and the bending strength, $\sigma_b$, are plotted as a function of the interlaminar fracture toughness for crack initiation. Interestingly enough, the bending modulus is practically independent of the interlaminar fracture toughness, while the bending strength display a tendency to increase as $G_{IC,NL}$ increases. The observed dependence of composite modulus and strength on the interlaminar fracture toughness closely resembles their dependence on the fibre–matrix adhesion. In fact, the observed behaviour is consistent with the existing literature on the effects of fibre–matrix adhesion on the quasi-static tensile and flexural mechanical properties of epoxy/graphite unidirectional composites. As reported by Madhukar and Drzal [50] and by Deng and Le [29] the fibre surface modification do not have much effect on the tensile and flexural moduli and on the fibre dominated properties. However, the strengths and the maximum strains, that are governed by the matrix and interface properties, are highly sensitive to the fibre surface modification. On the basis of our findings, similar considerations can be
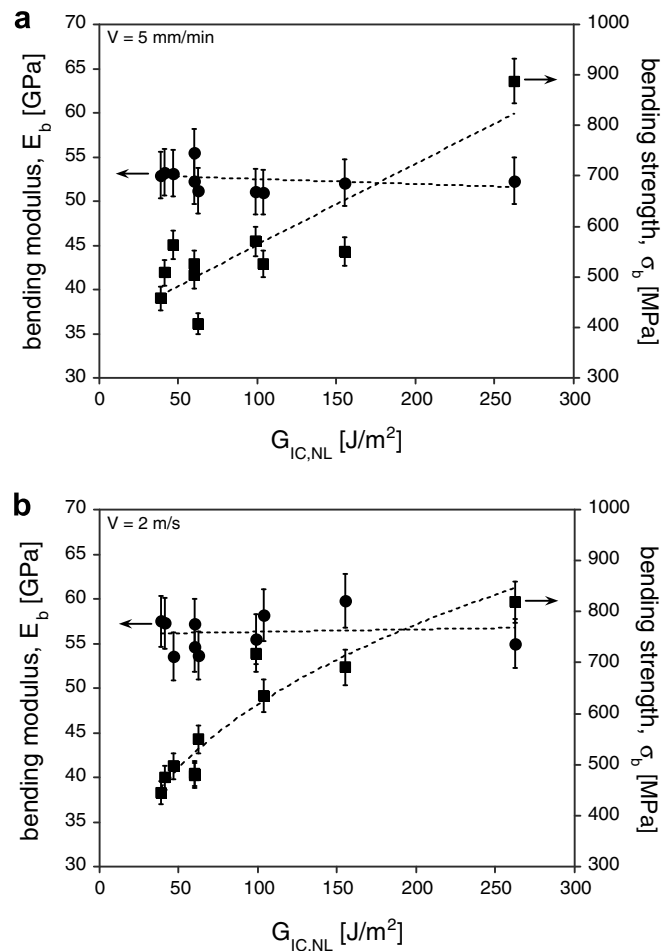


**Fig. 10.** Effect of the interlaminar fracture toughness ($G_{IC,NL}$) on the bending modulus ($\bullet$) and strength ($\blacksquare$) measured under (a) quasi-static (5 mm/min) and (b) impact (2 m/s) conditions.

put forward on the effect of interlaminar fracture toughness on the flexural properties of carbon/epoxy fabric laminates.

### 3.3. Impact resistance

The bending modulus, $E_b$, and the bending strength, $\sigma_b$, have been also evaluated under impact conditions by means of instrumented Charpy tests. The obtained values, plotted as a function of the interlaminar fracture toughness for crack initiation, are reported in Fig. 10b. It is interesting to note that, under impact conditions, both bending modulus and strength display a trend similar to that observed under quasi-static conditions. As expected, due to the viscoelastic behaviour of the PET interleaving foils and of the epoxy matrix, the stiffness and strength values of interleaved composites under impact conditions are higher than the corresponding data measured at a lower strain rate.

Fig. 11 documents the conditions of some of the investigated laminates after the Charpy impact test. It clearly emerges that the fracture behaviour under low speed impact conditions is profoundly affected by the interlaminar fracture toughness of the tested composites. For non-interleaved composites, that display the highest $G_{IC,NL}$ values, the broken specimens show a typically brittle aspect, with relatively sharp fracture surfaces and no (or very little) delamination damages (see Fig. 11a). When the interlaminar fracture toughness decreases, the failure process of the impacted specimens is characterized by progressively increasing delamination damage, and more extended fracture surfaces. For the lowest interlaminar fracture toughness values a certain disintegration of the tested specimens is also observed. Depending on the different fracture mechanisms, the load–displacement and energy–displacement curves recorded during the Charpy instrumented tests also markedly change with the interlaminar fracture toughness of the investigated laminates. By way of examples, the typical impact curves of two different laminates are reported in Fig. 12. It is evident that the brittle failure mode of non-interleaved composites (Fig. 12a) results in a load–displacement curve characterized by a sudden load drop with practically no energy consumed for the cracks propagation process. On the other hand, the load–displacement curve of interleaved composites displays a different trend, being a large amount of energy absorbed for damage delamination processes (Fig. 12b). For the case reported in Fig. 12b, which refers to an interleaved composite with a low (4.9%) ICA value, the total impact fracture energy exceeds by a factor of about 1.8 the energy absorbed by non-interleaved composites.

For each specimen, the total fracture energy ($E_T$) could be evaluated by measuring the total area under the curve and normalising it to the specimen cross sectional area. $E_T$ is the sum of a crack initiation energy ($E_I$) and a crack propagation energy ($E_P$). The initiation energy is the energy measured up to the first load drop, while the propagation energy is the energy required from this point to break the specimen. Total fracture, initiation, and propagation impact energies are summarised in Fig. 13 as a function of the interlaminar fracture toughness of the investigated laminates.
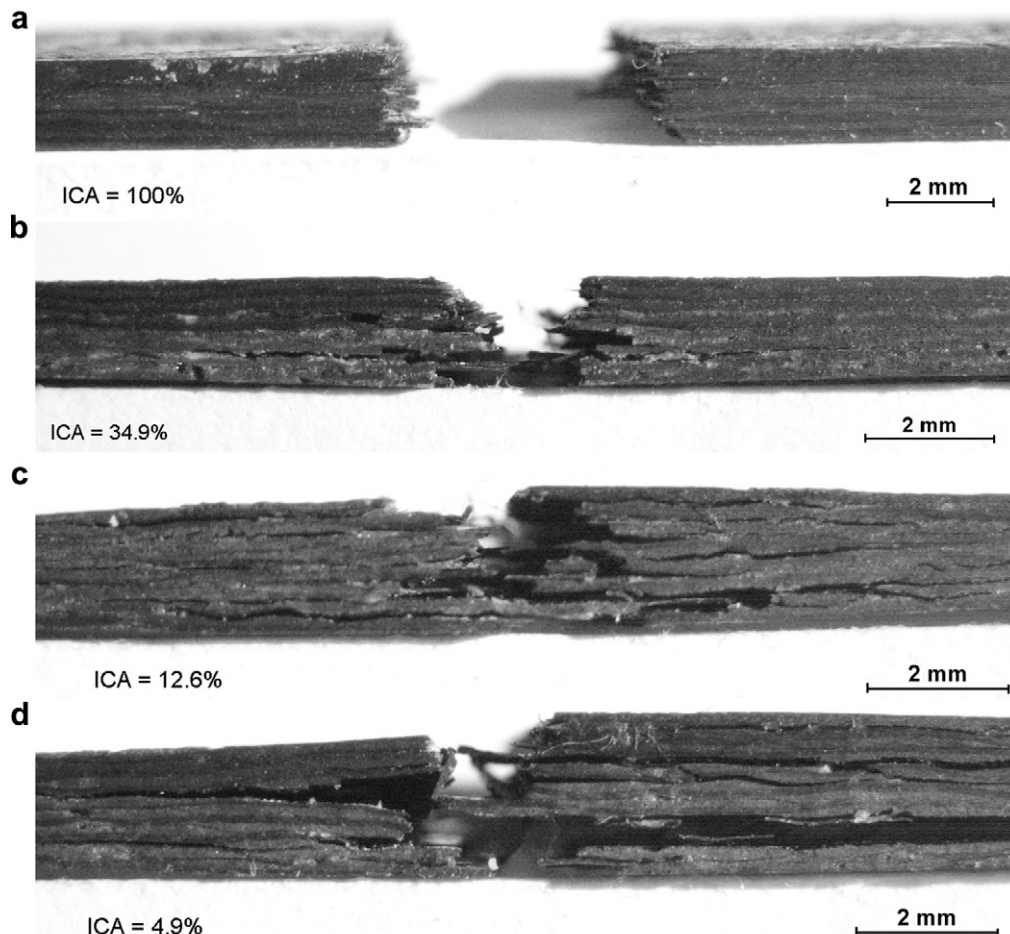


Fig. 11. Pictures of specimens after the Charpy impact test: (a) $G_{IC,NL}$ = 262 J/m$^2$ (ICA = 100%), (b) $G_{IC,NL}$ = 155 J/m$^2$ (ICA = 34.9%), (c) $G_{IC,NL}$ = 103 J/m$^2$ (ICA = 12.6%), and (d) $G_{IC,NL}$ = 62 J/m$^2$ (ICA = 4.9%).
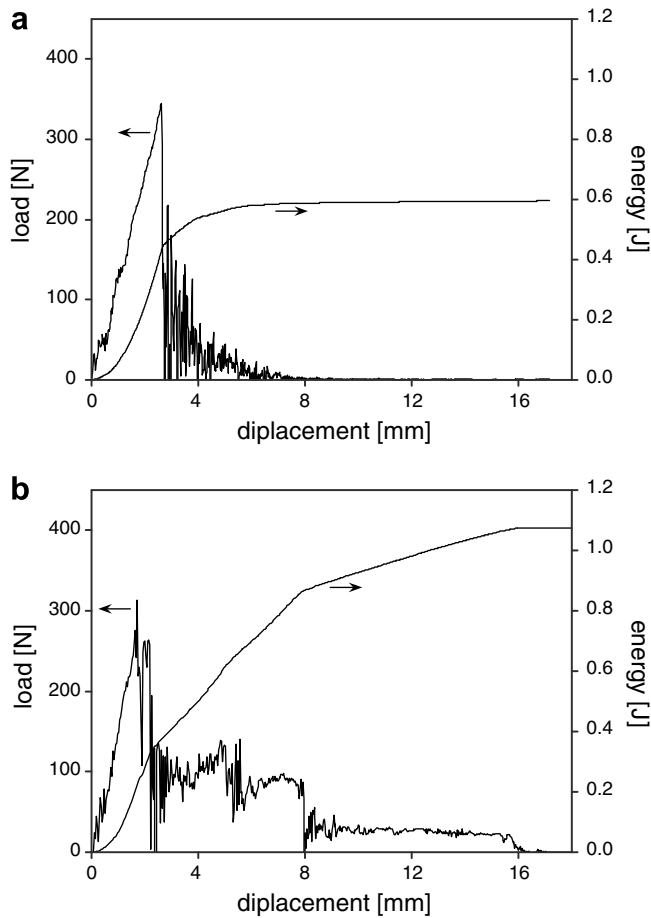
**Fig. 12.** Load–displacement and energy–displacement curves recorded during instrumented Charpy impact tests performed on composites with (a) $G_{IC,NL}$ = 262 J/m$^2$ (ICA = 100%), and (b) $G_{IC,NL}$ = 62 J/m$^2$ (ICA = 4.9%).
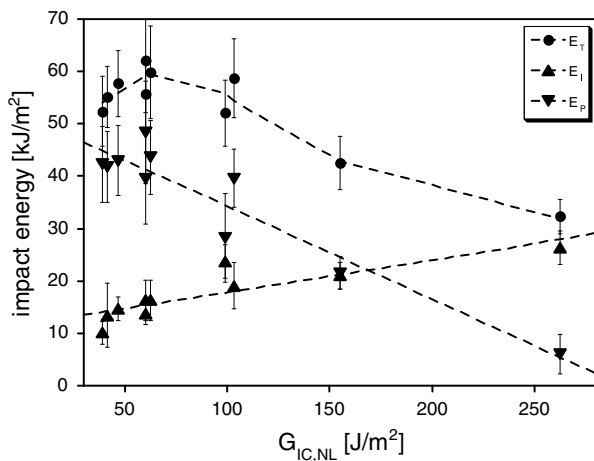


**Fig. 13.** Effect of interlaminar fracture toughness on the total fracture (●), on the initiation (▲), and on the propagation (▼) energies.

Interestingly enough, the interlaminar fracture toughness results to have an opposite influence on the initiation and propagation energies. In fact, while the initiation energy increases, the propagation energy decreases with the interlaminar fracture toughness. As a consequence, the total fracture energy passes through a maximum for a given $G_{IC,NL}$ value. The existence of an optimal value of the interlaminar fracture toughness, corresponding to maximum

energy absorption, can be explained by considering the occurrence of two concurrent phenomena. In fact, as the interfacial adhesion decreases the delaminated area increases. At the same time, as the interlaminar fracture toughness decreases, less and less energy is absorbed for creating a given delaminated area. These two phenomena have a contrasting effect on the fracture energy absorption process, thus justifying the existence of an optimal interlaminar adhesion value. This result has been theoretically predicted by numerical simulation of a layered beam under statically applied three point bending loads [37].

As a matter of fact, quite limited, and in some cases contrasting, experimental information exists on the role of interlaminar resistance on the impact behaviour of composite laminates. Bader et al. [51] observed that the principal effect of the interlaminar strength is to modify the mode of failure under impact conditions. On epoxy matrix unidirectional composites prepared with various both untreated and surface treated carbon fibres, they reported that at high levels of interlaminar strength a brittle failure occurred with relatively little absorbed energy. At low levels of strength they observed a multiple delamination, with an energy absorption about three times as high as in the brittle case, but with an extensive disintegration of the specimens. At intermediate values of interlaminar strength a progressive failure occurred which they consider to be the best practical compromise. Our results are in agreement with the above reported considerations. Also Yeung and Broutman [28] have shown that a non-monotonic correlation exists between the Charpy impact fracture energy and the interlaminar shear strength of epoxy and polyester–glass fabric laminates. The fibre–matrix interface adhesion was altered by surface treatments of the fabrics with silane coupling agents and with a silicone fluid mould release to achieve various interlaminar shear strengths (ILSS) in short-beam shear tests. The authors observed that with increasing ILSS the fracture initiation energy increased modestly, while the fracture propagation energy as well the total impact energy decreased exhibiting a minimum and levelling off at intermediate values.

Beaumont et al. [52] defined a dimensionless parameter called the ductility index (DI), which is found useful for ranking the impact performance of different materials under similar testing conditions. The DI is defined as the ratio between the propagation energy and the initiation energy, i.e.:

$$DI = \frac{E_P}{E_I}$$

High values of DI would mean that most of the total energy is expended for crack propagation. The ductility index values of the investigated laminates are reported in Fig. 14 as a function of the
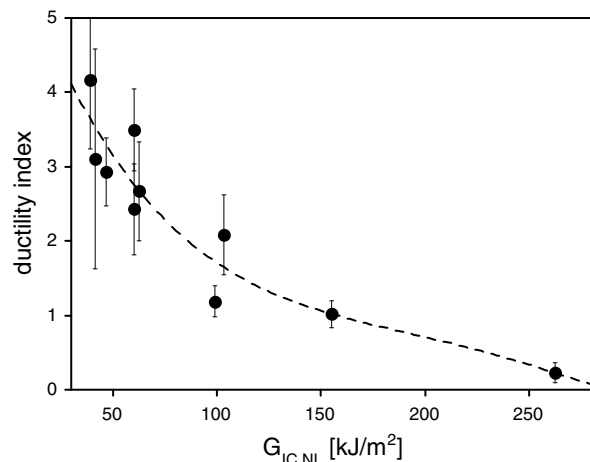


**Fig. 14.** Ductility index values as a function of the interlaminar fracture toughness.

interlaminar fracture toughness. Even if the data are affected by some scattering, they clearly show that the ductility index markedly increases as the interlaminar fracture toughness decreases. In particular, for the lowest explored value of the interlaminar fracture toughness the fracture propagation energy is almost four times higher that the fracture initiation component.

## 4. Conclusions

The Mode I interlaminar fracture toughness of carbon–epoxy laminates has been selectively varied, in the range from 40 up to 260 J/m$^2$, by interleaving with as-received and perforated PET foils. Its effect on quasi-static and impact mechanical response has been investigated by three point bending tests.

The following conclusions can be drawn:

(i) The bending modulus determined both under quasi-static and impact conditions is practically independent of the interlaminar fracture toughness.
(ii) The bending strength determined both under quasi-static and impact conditions markedly increase as the interlaminar fracture toughness increases.
(iii) The interlaminar fracture toughness has an opposite effect on the initiation and propagation energies under impact conditions. In fact, while the initiation energy increases, the propagation energy decreases with the interlaminar fracture toughness. As a consequence, the total fracture energy passes through a maximum for a given interlaminar fracture toughness value, for which the total impact energy increases is 1.8 times higher than the value observed for non-interleaved composites. The ductility index steadily increases from 0.2 up to 4.2 as the interlaminar fracture toughness decreases.

## Acknowledgments

## References

[1] Mallick PK. Fiber-reinforced composites: materials, manufacturing, and design. New York: Marcel Dekker, Inc.; 1993.
[2] Richardson MOW, Wisheart MJ. Review of low-velocity impact properties of composite materials. Compos Part A 1996;27(12):1123–31.
[3] Hancox NL. An overview of the impact behavior of fibre-reinforced composites. In: Reid SR, Zhou G, editors. Impact behaviour of fibre-reinforced composite materials and structures. Cambridge, UK: Woodhead Publishing Ltd.; 2000. p. 1–32.
[4] Johnson AF, Holzapfel M. Influence of delamination on impact damage in composite structures. Compos Sci Technol 2006;66:807–15.
[5] Larsson F. Damage tolerance of a stitched carbon/epoxy laminate. Compos Part A 1997;28(11):923–34.
[6] Kim JK, Mackay DB, Mai Y-W. Drop-weight impact damage tolerance of CFRP with rubber modified epoxy matrix. Composites 1993;24(6):485–94.
[7] Jang K, Cho W-J, Ha C-S. Influence of processing method on the fracture toughness of thermoplastic-modified, carbon-fiber-reinforced epoxy composites. Compos Sci Technol 1999;59(7):995–1001.
[8] Sjogren BA, Berglund LA. Toughening mechanisms in rubber-modified glass fiber/unsaturated polyester composites. Polym Compos 1999;20(5):705–12.
[9] Verrey J, Winkler Y, Michaud V, Manson J-AE. Interlaminar fracture toughness improvement in composites with hyperbranched polymer modified resin. Compos Sci Technol 2005;65:1527–36.
[10] Jain LK, Mai Y-W. In the effect of stitching on mode-I delamination toughness of laminated composites. Compos Sci Technol 1994;51(3):331–45.
[11] Jain LK, Mai Y-W. Determination of Mode II delamination toughness of stitched laminated composites. Compos Sci Technol 1995;55(3):241–53.
[12] Dransfield KA, Jain LK, Mai Y-W. On the effects of stitching in CFRPs—I. Mode I delamination toughness. Compos Sci Technol 1998;59(6):815–27.
[13] Jain LK, Dransfield KA, Mai Y-W. On the effects of stitching in CFRPs—II. Mode II delamination toughness. Compos Sci Technol 1998;59(6):829–37.
[14] Watt A, Goodwin AA, Mouritz AP. Thermal degradation of the mode I interlaminar fracture properties of stitched glass fibre vinyl ester composites. J Mater Sci 1998;33(10):2629–38.
[15] Yan WY, Liu HY, Mai Y-W. Mode II delamination toughness of z-pinned laminates. Compos Sci Technol 2004;64(13–14):1937–45.
[16] Cartie DDR, Troulis M, Partridge IK. Delamination of Z-pinned carbon fibre reinforced laminates. Compos Sci Technol 2006;66(6):855–61.
[17] Davidson BD, Hu H. Effect of interlayer modulus on fracture mode ratio for interleaved composite laminates. Eng Fract Mech 1995;52(2):243–53.
[18] Hillermeier RW, Seferis JC. Interlayer toughening of resin transfer molding composites. Compos Part A 2001;32:721–9.
[19] Jiang W, Y TFF, Tjong SC, Li RKY, Kim JK, Mai Y-W. Loading rate dependence of Mode II fracture behavior in interleaved carbon fibre/epoxy composite laminates. Appl Compos Mater 2001;8:361–9.
[20] Lee S-H, Noguchi H, Kim Y-B, Cheong S-K. Effect of interleaved non-woven carbon tissue on interlaminar fracture toughness of laminated composites: Part I – Mode II. J Compos Mater 2002;36(18):2153–67.
[21] Lee S-H, Noguchi H, Kim Y-B, Cheong S-K. Effect of interleaved non-woven carbon tissue on interlaminar fracture toughness of laminated composites: Part II – Mode I. J Compos Mater 2002;36(18):2169–81.
[22] Matsuda S, Hojo M, Ochiai S, Murakami A, Akimoto H, Ando M. Effect of ionomer thickness on mode I interlaminar fracture toughness for ionomer toughened CFRP. Compos Part A 1999;30:1311–9.
[23] Yun NG, Won YG, Kim SC. Toughening of carbon fiber/epoxy composite by inserting polysulfone film to form morphology spectrum. Polymer 2004;45:6953–8.
[24] Gao F, Jiao GQ, Lu ZX, Ning RC. Mode II delamination and damage resistance of carbon/epoxy composite laminates interleaved with thermoplastic particles. J Compos Mater 2007;41(1):111–23.
[25] Walker L, Sohn MS, Hu XZ. Improving impact resistance of carbon-fibre composites through interlaminar reinforcement. Compos Part A – Appl Sci Manufact 2002;33(6):893–902.
[26] Kim JK, Mai Y-W. Engineered interfaces in fibre-reinforced composites. Oxford: Elsevier Science Publishers; 1998.
[27] Wang TWH, Blum FD. Interfacial mobility and its effect on interlaminar fracture toughness in glass-fibre-reinforced epoxy laminates. J Mater Sci 1996;31(19):5231–8.
[28] Yeung P, Broutman LJ. The effect of glass–resin interface strength on the impact strength of fiber reinforced plastics. Polym Eng Sci 1978;18(2):62–72.
[29] Deng SQ, Ye L. Influence of fiber–matrix adhesion on mechanical properties of graphite/epoxy composites: I. Tensile, flexure, and fatigue properties. J Reinf Plast Compos 1999;18(11):1021–40.
[30] Madhukar MS, Drzal LT. Fiber–matrix adhesion and its effect on composite mechanical properties: IV. Mode I and Mode II fracture toughness of graphite/epoxy composites. J Compos Mater 1992;26(7):936–68.
[31] Goan JC, Martin TW, Prescott R. The influence of interfacial bonding on the properties of carbon fiber composites. In: 28th Annual Technical Conference Reinforced Plastic Composites Institute; 1973: SPI.
[32] Hong S, Liu D. On the relationship between impact energy and delamination area. Exp Mech 1989;29(2):115–20.
[33] Favre JP. Improving the fracture energy of carbon fiber reinforced plastics by delamination promoters. J Mater Sci 1977;12:43–50.
[34] Mai YW, Cotterell B, Lord R. On fiber composites with intermittent interlaminar bonding. In: ICCM-IV, progress in science and engineering of composites. Tokyo: North Holland Pub, Amsterdam; 1982.
[35] Jea LC, Felbeck DK. Increased fracture toughness of graphite–epoxy composites through intermittent interlaminar bonding. J Compos Mater 1980;14:245–59.
[36] Jang BZ, Lieu YK, Chung WC, Hwang LR. Controlled energy dissipation in fibrous composites, I. Controlled delamination. Polym Compos 1987;8:94–102.
[37] Lear MH, Sankar BV. Optimizing energy absorption in multi-layered materials through controlled delamination. J Mater Sci 1999;34(17):4181–91.
[38] Schoeppner GA, Abrate S. Delamination threshold loads for low velocity impact on composite laminates. Compos Part A – Appl Sci Manufact 2000;31(9):903–15.
[39] Fuoss E, Straznicky PV, Poon C. Effects of stacking sequence on the impact resistance in composite laminates – Part 1: parametric study. Compos Struct 1998;41(1):67–77.
[40] Pegoretti A, Guardini A, Migliaresi C, Ricco T. Recovery of post-yielding deformations in semi-crystalline poly(ethylene-terephthalate). Polymer 2000;41(5):1857–64.
[41] Davies P, Blackman BRK, Brunner AJ. Mode II delamination. In: Moore DR, Pavan A, Williams JG, editors. Fracture mechanics testing methods for polymers, adhesives and composites. Amsterdam: Elsevier; 2001. p. 307–33.
[42] Hojo M, Ando T, Tanaka M, Adachi T, Ochiai S, Endo Y. Modes I and II interlaminar fracture toughness and fatigue delamination of CF/epoxy laminates with self-same epoxy interleaf. Int J Fatigue 2006;28:1154–65.
[43] Naik NK, Reddy KS, Meduri S, Raju NB, Prasad PD, Azad SNM, et al. Interlaminar fracture characterization for plain weave fabric composites. J Mater Sci 2002;37:2983–7.
[44] Alvarez V, Bernal CR, Frontini PM, Vazquez A. The influence of matrix chemical structure on the Mode I and II interlaminar fracture toughness of glass-fiber/epoxy composites. Polym Compos 2003;24(1):140–8.

[45] Chen SF, Jang BZ. Fracture behavior of interleaved fiber resin composites. Compos Sci Technol 1991;41(1):77–97.

[46] Jordan W. Changing the toughness of graphite fiber/resin based composites by changing their internal structure. Compos Part B 2000;31:245–52.

[47] Mujika F, De Benito A, Fernadez B, Vazquez A, Llano-Ponte R, Mondragon I. Mechanical properties ofcarbon woven reinforced epoxy matrix composites. A study on the influence of matrix modification with polysulfone. Polym Compos 2002;23(3):372–82.

[48] Park SJ, Seo MK, Lee JR. Roles of interfaces between carbon fibers and epoxy matrix on interlaminar fracture toughness of composites. Compos Interfaces 2006;13(2-3):249–67.

[49] Stevanovica D, Kalyanasundaramb S, Lowe A, Jarc P-YB. Mode I and mode II delamination properties of glass/vinyl-ester composite toughened by particulate modified interlayers. Compos Sci Technol 2003;63:1949–64.

[50] Madhukar MS, Drzal LT. Fiber–matrix adhesion and its effect on composite mechanical properties: II. Longitudinal (0°) and transverse (90°) tensile and flexure behavior of graphite/epoxy composites.J Compos Mater 1991;25: 958–91.

[51] Bader MG, Bailey JE, Bell I. The effect of fibre–matrix interface strength on the impact and fracture properties of carbon-fibre-reinforced epoxy resin composites. J Phys D: Appl Phys 1973;6:572–86.

[52] Beaumont PWR, Reiwald PG, Zweben C. Methods for improving the impact resistance of composite materials. ASTM Special Tech Public 1974;568: 134–58.